Electrodynamics of unintentional wire antennas*

Larysa Kriuchkova[1,†], Nataliia Mazur[1,*,†], Ivan Tsmokanych[2,†], and Anatolii Holishevskyi[2,†]

[1] *Borys Grinchenko Kyiv Metropolitan University, 18/2 Bulvarno-Kudriavska str., 04053 Kyiv, Ukraine*
[2] *State Research Institute of Cyber Security and Information Protection, 3/6 Maksyma Zaliznyaka str., 03142 Kyiv, Ukraine*

Abstract

The urgency of protecting information at information facilities from leakage via technical channels is undeniable and ranks among the leading areas of information security. The rapid growth of technical capabilities for intercepting and generating information leaks through technical channels is driving increased demand for information security methods and tools. Therefore, theoretical and practical issues related to the study of electrodynamic processes in information systems are highly relevant. This paper presents original results from studies of electrodynamic processes in unintentional wire antennas to ensure electromagnetic compatibility and information protection at information facilities sites. An iterative method for determining current in a curved wire is considered, and formulas for determining the electromagnetic field generated by a wire radiator in the near field are presented. Distributions of electric and magnetic field strengths for a corner radiator are shown. Original results of a study of electrodynamic processes in the near field of loop antennas are presented. The calculated spatial values of the magnetic induction vector of a loop antenna at different distances from the frame plane are given. It is proposed to experimentally determine the spatial characteristics of the near field of wire antennas by introducing passive electric oscillatory circuits tuned to the field frequency at specific points in space. The practical significance of the results lies in their applicability across various industries for determining the spatial characteristics of the near field of unintentional wire antennas, as well as for the synthesis of systems whose structure includes wire and, in particular, loop antennas.

Keywords

unintentional antenna, unintentional wire antennas, TEMPEST, electromagnetic compatibility and security, electrodynamic process, iterative method, magnetic induction vector

1. Introduction

The rapid development of computing technology in the modern world has opened up opportunities for automating mental work and enabled the creation of new information technologies. The unlawful falsification or distortion, destruction, or disclosure of certain classified information causes serious harm to participants in automated information exchange processes.

When addressing the issue of information security, the object of information activity should be considered as a complex, dynamic, multi-parameter, weakly deterministic system with distributed parameters, in which, as a result of internal electromagnetic interactions and external intelligence threats, unexpected emergent properties may arise, manifesting in the formation of dangerous signals [1, 2]. Obviously, to achieve the required level of information security, the ability to predict and prevent the occurrence of emergent properties at the protected object must be ensured.

The physical nature of technical intelligence stems from the fact that processes associated with the processing, transmission, and storage of information generate side effects: scattered fields of various physical natures and the induction of currents and voltages in non-informational physical circuits. The growing technical capabilities for intercepting information through technical leakage channels and for generating such leaks are driving increasing demands for information security methods and tools, making theoretical and practical issues related to the study of electrodynamic processes in information systems highly relevant [3].

* *CSDP'2026: Cyber Security and Data Protection, February 12, 2026, Lviv, Ukraine*
* Corresponding author.
† These authors contributed equally.
l.kriuchkova@kubg.edu.ua (L. Kriuchkova); n.mazur@kubg.edu.ua (N. Mazur); ivakobor@ukr.net (I. Tsmokanych); 380937029549@ukr.net (A. Holishevskyi)
0000-0002-8509-6659 (L. Kriuchkova); 0000-0001-7671-8287 (N. Mazur); 0000-0002-5085-8457 (I. Tsmokanych); 0000-0001-9981-7771 (A. Holishevskyi)

An adequate assessment of the likelihood of a potential security breach depends on expert knowledge of radio frequency technology, particularly the associated causal factors and their interrelationships. The literature has identified several factors that can cause unintentional electromagnetic emissions, leading to information security breaches [4, 5].

In [6], the authors describe the problems caused by four types of electromagnetic radiation from displays, keyboard inputs, printed information, and communication data. In [7], the authors consider the interception and security risks of wireless keyboard signals, regardless of communication protocols, noise, and physical obstacles. Printers as sources of unintentional electromagnetic radiation are discussed in [8—11]. The use of commercial printers connected via a local area network is quite common for printing large volumes of data in office settings. These printers are usually equipped with various components such as hard drives, power and signal lines, connectors, and wireless transceivers. Measuring the electromagnetic radiation near the printer enables recovery of printed data. In [12], unintentional radiation from an unshielded twisted cable caused by the twisting structure is discussed.

Electromagnetic signal leakage from various sources via signal lines, power lines, telephone lines, and water pipes can also cause numerous safety issues [13]. The primary concern in such scenarios is the characteristics of conductors acting as antennas at high frequencies. Important considerations for the electrical dynamics of long-distance power transmission lines and internal power distribution systems are needed to address electromagnetic interference [14, 15].

The literature contains very limited information on both the spatial structure of the near field of specific types of antennas and the general patterns (the main one being the nature of amplitude change) inherent in the electromagnetic field of arbitrary antennas when moving from the far zone to the intermediate zone and, especially, to the near zone [16, 17].

The purpose of the article is to study electrodynamic processes in unintentional wire antennas to solve problems of ensuring electromagnetic compatibility and information protection at information facilities.

2. An iterative method for determining the current in a curved wire

The wire radiator is geometrically defined by its shape and parameters—length l and radius a (thickness 2a) with the ratio

$$a \ll l \text{ and } a \ll \lambda. \tag{1}$$

The field of wire electrodynamic structures is determined by the current in the wire as a function $I(\xi)$ of the coordinate ξ в along the wire.

Figure 1 shows a rectilinear (a), curved (b), two-wire (c), and frame (d) wire radiators, each of which is located in the primary field E^n of a plane incident wave.

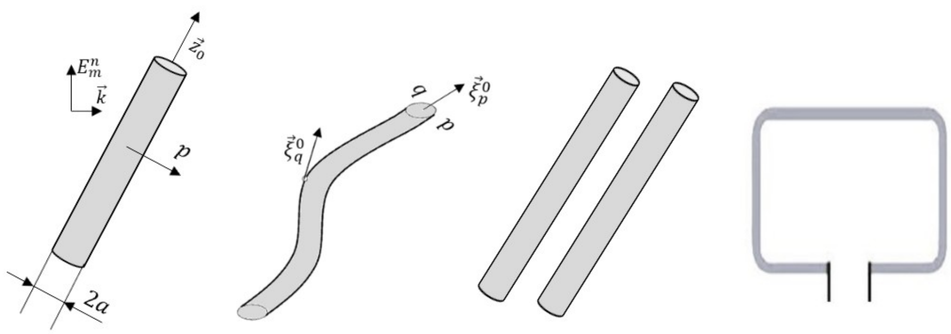

a) b) c) d)

Figure 1: Types of wire electrodynamic structures:
(a) straight section, (b) curved wire, (c) two wires, (d) frame

Fulfilment of inequalities (1) allows us to neglect the transverse components of the surface current density in the initial formulation in comparison with the longitudinal ones, and also to find the field of the wire by the average longitudinal density on the circumference of the cross-section, i.e., by the current $I(\xi)$ and the linear charge $\tau(\xi)$ of the wire

$$\begin{aligned} a\int_0^{2\pi} H_{\varphi m}(\xi,\varphi)\,d\varphi = I(\xi), \\ a\varepsilon\int_0^{2\pi} E_{\rho m}(\xi,\varphi)\,d\varphi = \tau(\xi). \end{aligned} \tag{2}$$

Integration in (2) is only over the angular coordinate φ means that in each cross-section of the curved wire a local system of cylindrical coordinates ρ, φ, z is introduced, and the transition from a rectilinear wire (Figure 1a) to a curvilinear one (Figure 1b) will lead, under the conditions of fulfillment of (1), only to a formal replacement $z \rightarrow \xi$.

The following relationships between current and charge are known [18]

$$-\frac{dI(\xi)}{d\xi} = j\varpi\tau(\xi) \tag{3}$$

$$\frac{d\tau(\xi)}{d\xi} = -j\varpi\mu\varepsilon I(\xi) + f(\xi) \tag{4}$$

where $f(\xi)$ is the characteristic of the surface field of the wire, equal to

$$f(\xi) = \varepsilon a\int_0^{2\pi} (E_{\xi m})'_{\rho}\,d\varphi = 2\pi a\varepsilon (E_{\xi m\,av})'_{\rho} \tag{5}$$

at $\rho = a$, i.e., coinciding up to a constant factor $2\pi a\varepsilon$ with the derivative along the normal from the average value of the tangential component of the electric field strength on the surface of the wire.

In (3) and (4), the variables$I(\xi)$, $\tau(\xi)$ completely characterize the behavior of the wire in an electromagnetic field.

The functions $I(\xi)$, $\tau(\xi)$ are described by ordinary differential equations

$$I''_{\xi} + k^2 I = -j\varpi f(\xi), \tag{6}$$

$$\tau''_{\xi} + k^2\tau = f'_{\xi}. \tag{7}$$

The formal solution of equation (6) consists of two terms of the current $I_h + I_{\mathrm{in}\,h} = I$ as solutions of the homogeneous and non-homogeneous equations (6)

$$I_h = C_1\cos k\xi + C_2\sin k\xi \tag{8}$$

$$I_{\mathrm{in}\,h} = -j\frac{\varpi}{k}\int_{\xi_0}^{\xi} f(\xi')\sin k(\xi-\xi')\,d\xi',\ \xi_0 \le \xi \le \xi_L, \tag{9}$$

where ξ_0 and $\xi_L$correspond to the beginning and end of the wire, and when substituting (9) into (6), one should use the well-known formula $q(\xi)$

$$\frac{d}{d\xi}\int_{p(\xi)}^{q} \psi(\xi,\xi')\,d\xi' = \int_p^q \frac{d\psi}{d\xi}\,d\xi' + \psi(q,\xi)\,q'_{\xi} - \psi(p,\xi)\,p'_{\xi}. \tag{10}$$

The importance of the resulting formula (9) lies in its ability to solve the inverse problem of determining the current from the field for a wire radiator. In particular, this makes it possible to organize an iterative process for finding the current in wire antennas.

The pair of relations (6), (9) can be used to mutually establish the relationship between the current and the surface characteristic. According to (5), the characteristic $f(\xi)$ is determined by both the primary and secondary fields created by the current in the wire

$$f=f^{pr}+f^{s}=2\pi a\varepsilon\left(E_{\xi m\,av}^{pr}\right)_{\rho}^{'}+2\pi a\varepsilon\left(E_{\xi m\,av}^{s}\right)_{\rho}^{'}. \tag{11}$$

Formula for f, taking into account the boundary condition on the surface of the wire

$$E_{\xi m\,av}(a)=E_{\xi m\,av}^{pr}(a)+E_{\xi m\,av}^{s}(a)=0. \tag{12}$$

Using the usual definition of the derivative in (10)

$$f=2\pi a\varepsilon\lim_{\rho\to a}\frac{E_{\xi m\,av}(\rho)-E_{\xi m\,av}(a)}{\rho-a} \tag{13}$$

and substituting (11) into (12), we have the characteristic

$$f_{\Gamma}(\xi)=2\pi\varepsilon\lim_{\rho\to a}\frac{a\left[E_{\xi m\,av}^{s}(\rho,\xi)+E_{\xi m\,av}^{pr}(\rho,\xi)\right]}{\rho-a} \tag{14}$$

related to an ideal wire. Substituting (14) into (9) yields a formula for the current $I_{\text{in}\,h}$, taking into account the boundary condition (12), which allows us to interpret (9) as an integral equation of the problem.

From (11) and (9) it follows that the current $I_{\text{in}\,h}$ consists of two currents

$$I_{\text{in}}^{pr}=-2\pi a\varepsilon\frac{j\varpi}{k}\int_{\xi_0}^{\xi}\left(E_{\xi m\,av}^{pr}\right)_{\rho}^{'}\sin k\left(\xi-\xi^{'}\right)d\xi^{'}, \tag{15}$$

$$I_{\text{in}}^{s}=-2\pi a\varepsilon\frac{j\varpi}{k}\int_{\xi_0}^{\xi}\left(E_{\xi m\,av}^{s}\right)_{\rho}^{'}\sin k\left(\xi-\xi^{'}\right)d\xi^{'} \tag{16}$$

where the determination of I_{in}^{pr} according to (15) is carried out using a given primary field. The situation is different with the current I_{in}^{s}, the determination of which according to (16) requires a preliminary calculation of the secondary field at the surface of the wire.

It is of interest to establish the conditional distribution of the roles of currents (8), (15), and (16) in the creation of a secondary field, although the root cause of all three currents is the primary field E^{pr}. According to (8), for a known type of current I_h, the constants C_1, C_2 are determined by the length of the wire L and the end values of the currents I_{in}^{pr}, I_{in}^{s}, if we introduce the condition of equality to zero of the total current at the ends of the wire

$$C_1\cos k\xi_0+C_2\sin k\xi_0=-\left[I_{\text{in}}^{pr}(\xi_0)+I_{\text{in}}^{s}(\xi_0)\right], \tag{17}$$

$$C_1\cos k\xi_L+C_2\sin k\xi_L=-\left[I_{\text{in}}^{pr}(\xi_L)+I_{\text{in}}^{s}(\xi_L)\right]. \tag{18}$$

According to (15), the current I_{in}^{pr} is zero for an infinitely thin wire $(a\to 0)$, i.e., the influence of the wire thickness is primarily taken into account by I_{in}^{pr}. The role of the current I_{in}^{s} is more complex, since it does not vanish even when $a\to 0$, since in (16) the integrand tends to ∞.

Let us assume the opposite, that $\left(E_{\xi m}^{s}\right)_{\rho}^{'}$ does not have a singularity of the type a^{-1}. Then, by virtue of (15), for an infinitely thin wire $I_{\text{in}}^{s}\to 0$, which together with $I_{\text{in}}^{pr}\to 0$, according to (17), (8), for a wire of finite length $(\xi_0\neq\xi_L)$ also gives zero current $I_h=0$. Reality refutes this result, since even in an infinitely thin wire a current is induced due to the primary field, which, it turns out, cannot consist only of I_h, but is supplemented by current I_{in}^{s} according to (16).

Further analysis of (14) is useful for developing an iterative algorithm for finding the current $I_{\mathrm{in}\,h}$. According to the classical interpretation, the limit in (14) exists if the numerator is proportional to the value of ρ-a, i.e., for the near-surface field

$$E^{s}_{\xi m\,av}(\rho,\xi)=-E^{pr}_{\xi m\,av}(\rho,\xi)+\mathcal{E}(\xi)(1-\frac{\rho}{a}) \tag{19}$$

where the function $\mathcal{E}(\xi)$ does not depend on ρ. Finding this function, as well as the current $I(\xi)$, allows us to consider the electrodynamic problem solved, and

$$f_{\Gamma}(\xi)=-2\pi\xi\,\mathcal{E}(\xi). \tag{20}$$

The iterative process is based on the following assumption. The secondary field near a wire is primarily determined by the nearest section of the wire carrying current and only to a second approximation by the integral effect of the remaining sections of the wire. This assumption is supported not only by the weakening of the influence with distance, but also by the presence of a compensating effect, since the wire is electrically neutral and therefore carries charges of both signs.

So, as a first approximation in (19), (20) it is proposed to set

$$\begin{gathered}\mathcal{E}(\xi)\approx E^{pr}_{\xi m\,av}(a),\\ E^{s}_{\xi m\,av}\approx -E^{pr}_{\xi m\,av}\rho/a,\\ f_1=-2\pi\varepsilon E^{pr}_{\xi m\,av}.\end{gathered} \tag{21}$$

Substituting (21) into (9), and then (8), (9) into (17) allows us to find the total current of the wire in the first approximation $I_1=I_{h1}+I_{\mathrm{in}\,h1}$.

To find the second approximation of the characteristic $f_2(\xi)$, the field near the wire with the found current $I_1(\xi)$is calculated. We use a linear integral of the type (21) of the dipole field

$$E^{s}(q)=\int_{\xi_0}^{\xi_L}[I_h(\xi_p)+I_{\mathrm{in}\,h}(\xi_p)]G_{pq}\,d\xi_p, \tag{22}$$

where

$$G_{pq}=(j\varpi\varepsilon)^{-1}[k^2 G_{pq}\vec{\xi}^0_p+grad_q\,\mathrm{div}_q(G_{pq}\vec{\xi}^0_p)] \tag{23}$$

where $\vec{r}_p=\vec{x}_0(x)(\xi_p)+\vec{y}_0 y(\xi_p)+\vec{z}_0 z(\xi_p)$ is the radius vector of a point p lying on the centerline of the wire. We find the tangent component of vector (19) at a point q on the surface of the wire (Figure 1b)

$$\xi^{s}_{\xi m}(q)=\vec{\xi}^0_p\cdot E^{s}_q=\int_{\xi_0}^{\xi_L}(I_h+I_{\mathrm{in}\,h})\times K_{pq}\,d\xi_p \tag{24}$$

where

$$K_{pq}=\vec{\xi}^0_p\cdot G_{pq}. \tag{25}$$

To simplify the calculations, we supplement inequalities (1) with the condition that the tangent unit vector $\vec{\xi}^0_p$ is independent of the position of the point q within the contour of a single cross-section. This allows us to preserve the form (1) when finding the average stress by substituting the quantity K_{pq}

$$K^{av}_{pq}=\frac{1}{2\pi}\int_0^{2\pi}\vec{\xi}^0_q\cdot G_{pq}\,d\varphi_q=\frac{1}{2\pi}\vec{\xi}^0_q\cdot\int_0^{2\pi}G_{pq}\,d\varphi_q=\vec{\xi}^0_q\cdot G^{av}_{pq}. \tag{26}$$

After the tangential component of the field strength near the conductor is determined using (22) and (23), the characteristic $f_2(\xi)$ is found either using (14) or (18) and (19). Substituting $f_2(\xi)$ into (9) and taking into account (8) and (17) yields the conductor current in the second approximation: $I_2 = I_{h2} + I_{\text{in}\,h2}$. The iterative process considered is convergent, and there is reason to believe that in most cases a third approximation of the conductor current will not be necessary, as it differs little from I_2.

3. Spatial characteristics of the near field of power supply wires in a data transmission system

The results of the study of the electromagnetic field in the near zone created by a curved wire with a given current distribution are presented in [19].

The near-field zone of power lines transmitting information is characterized by the presence of all field components, an irregular field, and the complex nature of the Poynting vector. Since the near-field zone contains not only active but also reactive energy, calculations should be performed in a general manner, taking into account all field components [20].

The field distribution calculation was performed for the case where data is transmitted at a frequency along a right-angled wire with a leg length of a = 5 m and a wire diameter significantly smaller than the wavelength $d < \lambda$. This value was chosen because this frequency is close to the frequency range used by amateur radio stations (28.0–29.7 MHz), which, according to the National Table of Radio Frequency Band Allocations of Ukraine, can be used for experimental research in addition to communications between amateur radio stations [21].

The current distribution is assumed to be uniform along the length of the wire. As is known [20], the amplitudes of the electric and magnetic fields depend linearly on the amplitude of the current flowing along the wire. For the wire structure under consideration, normalized distributions of the electric $E(x,y,z)$and magnetic $H(x,y,z)$ field strengths for frequency were constructed f = 30 MHz (Figures 2a and 2b).

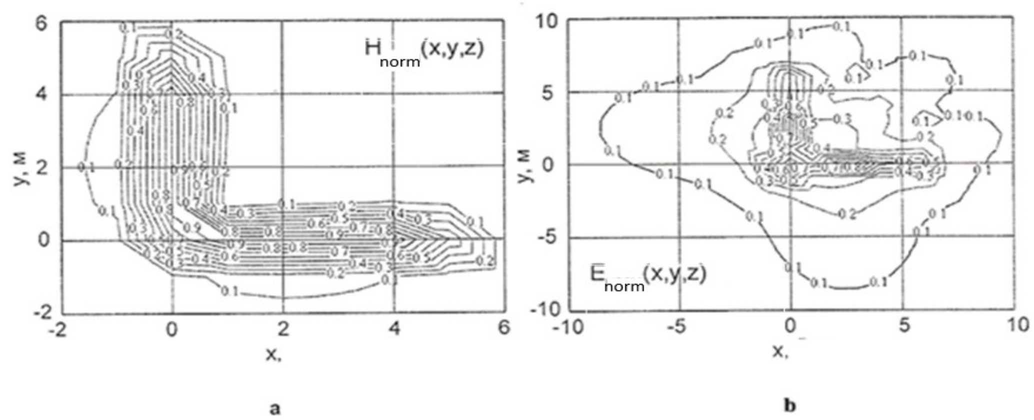

Figure 2: Distribution of normalized intensities of (a) magnetic $H(x,y,z)$ and (b) electric $E(x,y,z)$fields of a wire bent at a right angle for frequency f = 30 MHz

The graphs show that the distribution of electric $E(x,y,z)$ and magnetic $H(x,y,z)$ field strengths follows the geometry of the wire. As the distance from the observation point to the emitter increases, the electric field strength $E(x,y,z)$ contours that follow the conductor's geometry become smoother. As the strengths generated by each arm are added together, additional maxima appear between them. As the distance from the wire increases further, the level lines smooth out, assuming a spherical shape. Compared to the electric field strength $E(x,y,z)$, the magnetic field amplitude $H(x,y,z)$ decreases more rapidly with increasing distance from the wire, but the amplitude decreases unevenly: it decays faster on the inner side of the wire than on the outer side (see Figure 2a).

The distribution of the radiation power density of a wire bent at a right angle at a frequency f = 30 MHz shown in Figure 3 follows the contours of a corner wire.

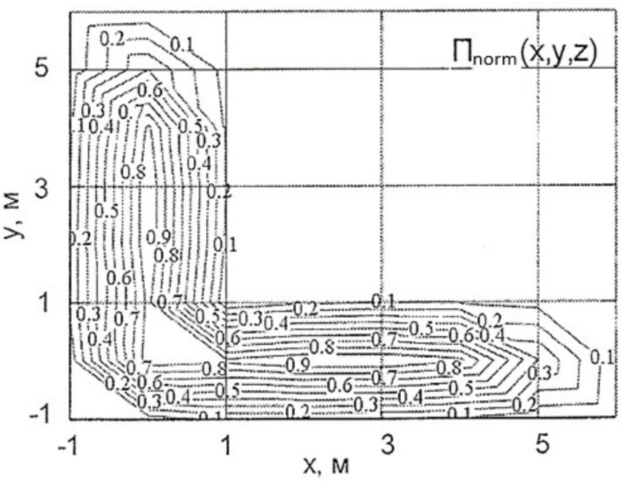

Figure 3: Distribution of the radiation power density of a wire bent at a right angle for the frequency f = 30 MHz

The Poynting vector is found as the vector product of the complex amplitudes of the electric and magnetic field strengths [20], therefore its distribution follows the distribution of the magnetic field strength and decreases with increasing distance from the wire under consideration to the observation point.

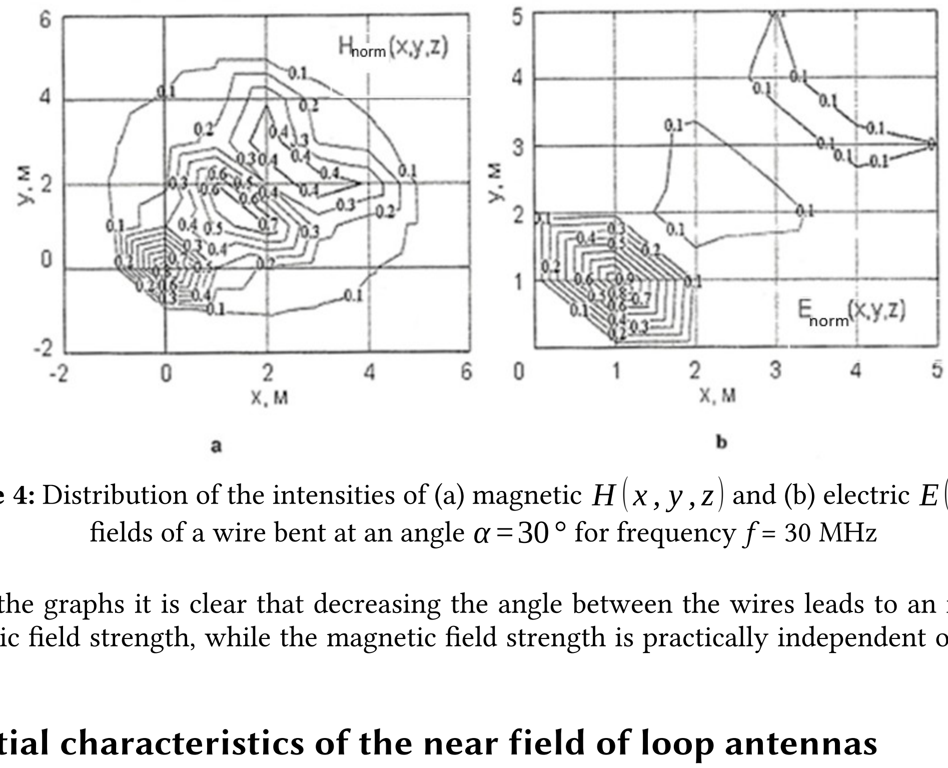

Figure 4: Distribution of the intensities of (a) magnetic $H(x,y,z)$ and (b) electric $E(x,y,z)$ fields of a wire bent at an angle $\alpha=30°$ for frequency f = 30 MHz

From the graphs it is clear that decreasing the angle between the wires leads to an increase in the electric field strength, while the magnetic field strength is practically independent of the angle α.

4. Spatial characteristics of the near field of loop antennas

The magnetic field of an inductive source current can be calculated as the vector sum (superposition) of the fields created by individual elementary sections of currents (Beau-Savart-Laplace law)

$$d\bar{B}=\frac{\mu_0}{4\pi}\frac{I_1[d\bar{l},\bar{r}]}{r^3} \tag{27}$$

where $d\bar{l}$ is a vector of a conductor element of length dl, drawn in the direction of current flow (Figure 1); $\bar{r}$ is a radius vector drawn from this conductor element to a given point in space; $\mu_0 = 4\pi \cdot 10^{-7} \left(\frac{Hn}{m}\right)$ is magnetic constant [20].

Considering that the dimensions of the field source are much smaller than the wavelength (the system is quasi-stationary), the phase delay can be neglected.

Magnetic induction vector modulus (Figure 5)

$$\overline{B}_0 = \frac{\mu_0 I_1 W_1}{4\pi} \oint \frac{\sin\alpha \sin\beta}{r^2} dl \tag{28}$$

where I_1 is the current value in the frame, W_1 is number of turns of the frame, α is angle between vectors $d\bar{l}$ and $\bar{r}$; β is angle between vectors $d\overline{B_0}$ and $d\overline{B_{0II}}$.

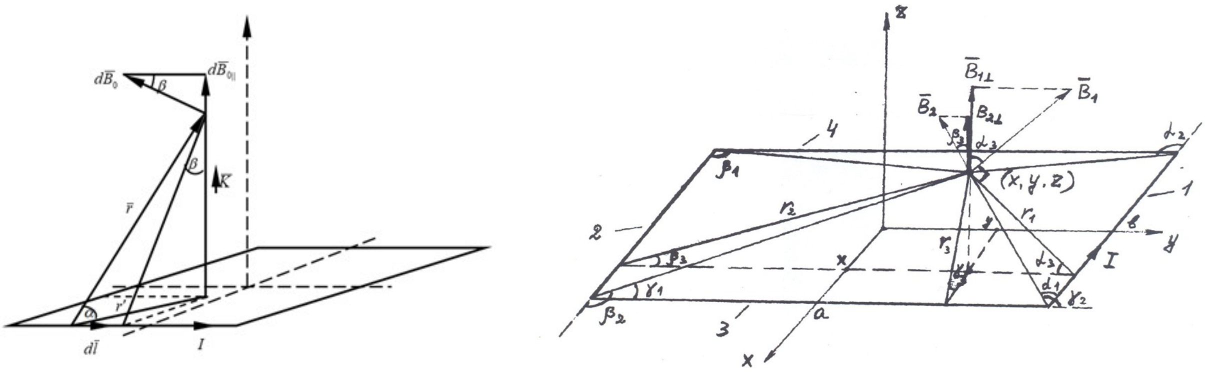

a b

Figure 5: Design schemes of the near field of a frame antenna:
(a) general and (b) along the sides of the frame

We have determined the spatial distribution of the values of the magnetic induction vector of a loop antenna measuring 0.7×0.6 m (Figure 6) [22]. As can be seen from Figures 6–9, with increasing distance from the frame plane, the field pattern becomes more uniform.

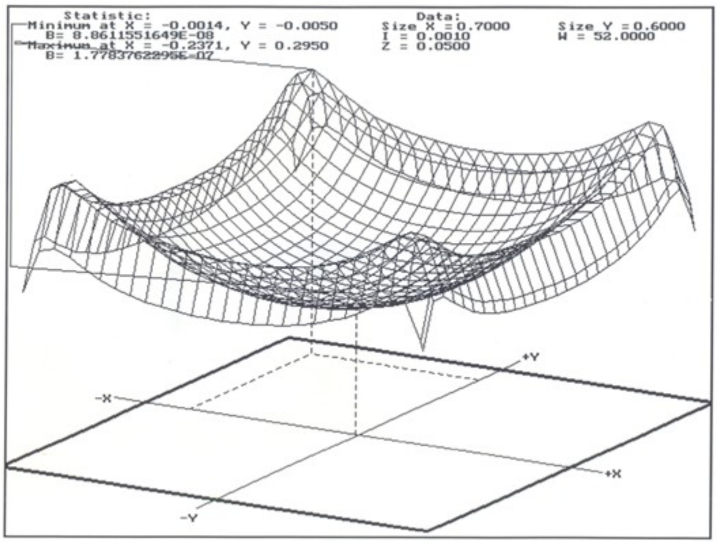

Figure 6: Spatial distribution of the values of the magnetic induction vector of a loop antenna at a distance of 0.05 m from the plane of the loop

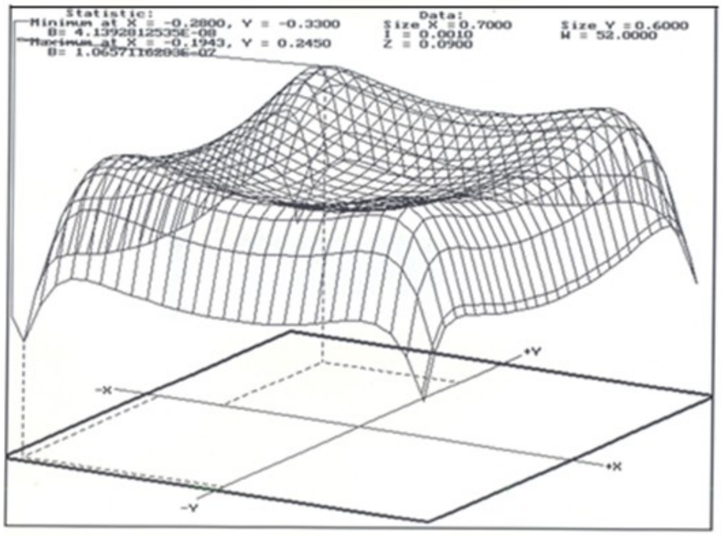

Figure 7: Spatial distribution of the values of the magnetic induction vector of a loop antenna at a distance of 0.09 m from the plane of the loop

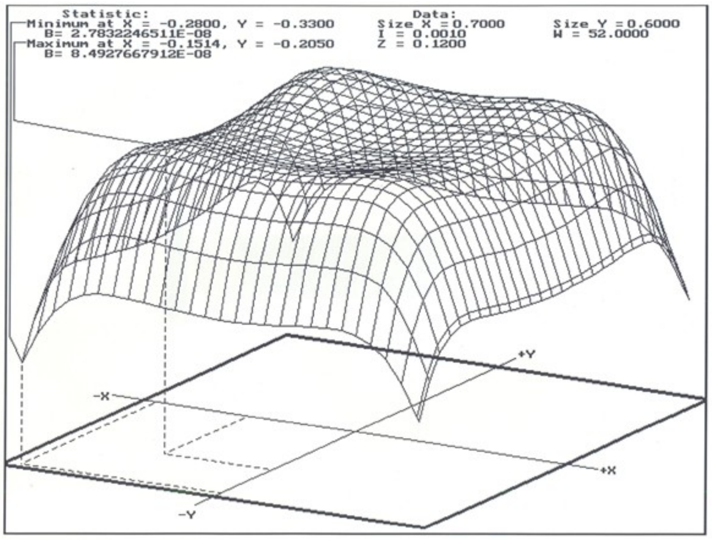

Figure 8: Spatial distribution of the values of the magnetic induction vector of a loop antenna at a distance of 0.12 m from the plane of the loop

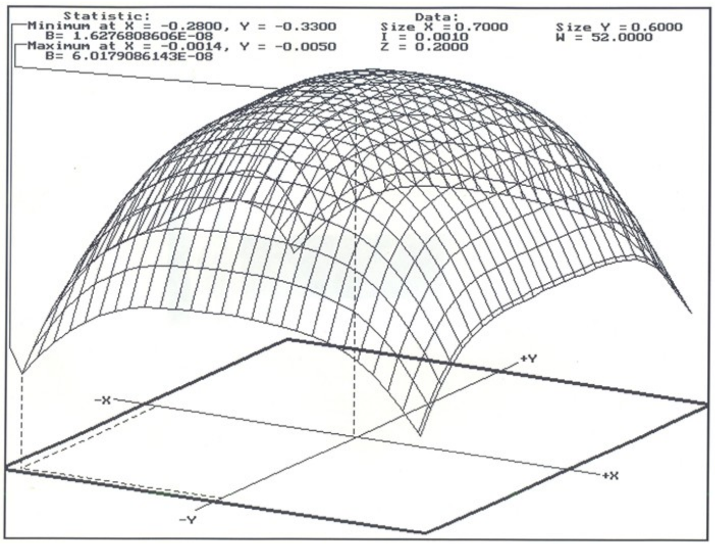

Figure 9: Spatial distribution of the values of the magnetic induction vector of a loop antenna at a distance of 0.2 m from the plane of the loop

In [22] it is proven that the spatial characteristics of the near-field of loop antennas can be determined experimentally by introducing passive electric oscillatory circuits tuned to the field frequency into given points in space. The obtained results are also relevant to broader radio channel security studies, where the analysis of electromagnetic propagation, signal characteristics, and technical leakage conditions is considered an important component of protecting wireless and information-processing systems [23]. Related studies on cooperative V2X-based UAV detection also show that distributed radio-frequency observations can improve the detection of low-power wireless objects and support more resilient monitoring of radio environments [24].

5. Conclusions

The iterative method of determining the current in a curved wire allows studying electrodynamic processes in unintended wire antennas. Considered distributions of electric and magnetic field strengths of curved wire emitters can be used to estimate the level of electromagnetic radiation that occurs when using electric wires for signal transmission, when organizing local networks and broadband access to the Internet.

The considered method of calculating and visualizing the spatial values of the magnetic induction vector of loop antennas can be used in the synthesis of systems that incorporate loop antennas, and in conducting research in information technologies and technical information protection, and in solving problems of electromagnetic compatibility of technical systems and electromagnetic safety.

Experimentally, the spatial characteristics of the near field of wire antennas can be determined by introducing passive electrical oscillatory circuits tuned to the field frequency into given points in space.

A promising direction for further research is the improvement of analytical and experimental methods for determining the spatial characteristics of wire antennas of complex configuration.

Declaration on Generative AI

While preparing this work, the authors used the AI programs Grammarly Pro to correct text grammar and Strike Plagiarism to search for possible plagiarism. After using this tool, the authors reviewed and edited the content as needed and took full responsibility for the publication's content.

References

[1] L. Kryuchkova, A Systematic Approach to Solving the Problem of Information Protection at the Objects of Information Activity, Inf. Secur. 2 (6) (2011) 5–7.

[2] V. Astapenya, et al., Analysis of Ways and Methods of Increasing the Availability of Information in Distributed Information Systems, in: 2021 IEEE 8th Int. Conf. on Problems of Infocommunications, Science and Technology, 2021. doi:10.1109/picst54195.2021.9772161

[3] L. Kriuchkova, V. Sokolov, P. Skladannyi, Determining the Zone of Successful Interaction in RFID Technologies, in: IEEE 29th Int. Seminar/Workshop on Direct and Inverse Problems of Electromagnetic and Acoustic Wave Theory, 2024, 168–171. doi:10.1109/diped63529.2024.10706153

[4] S. Vasylyshyn, I. Opirskyy, Combat Drone Swarm System (CDSS) based on Solana Blockchain Technology, in: 7th Int. Workshop on Computer Modeling and Intelligent Systems (CMIS), vol. 3702 (2024) 179–191.

[5] O. Harasymchuk, et al., Modern Methods of Ensuring Information Protection in Cybersecurity Systems using Artificial Intelligence and Blockchain Technology, Technology Center PC, 2025. doi:10.15587/978-617-8360-12-2

[6] Y. Suzuki, M. Masugi, K. Tajima, H. Yamane, Countermeasures to Prevent Eavesdropping on Unintentional Emanations from Personal Computers, NTT Tech. Rev. 6 (2008) 269–286.

[7] S. Jovanovic, et al., Security of Wireless Keyboards: Threats, Vulnerabilities and Countermeasures. Vojnoteh. Mil. Tech. Cour. 71 (2023) 296–315.
[8] I. Kubiak, J. Loughry, LED Arrays of Laser Printers as Valuable Sources of Electromagnetic Waves for Acquisition of Graphic Data, Electron. 8 (2019) 1078.
[9] S. Huzurbazar, D. Kuang, L. Lee, Landmark-based Algorithms for Group Average and Pattern Recognition, Pattern Recognit. 86 (2019) 172–187.
[10] J. I. Toledo, M. Carbonell, A. Fornés, J. Lladós, Information Extraction from Historical Handwritten Document Images with a Context-Aware Neural Model, Pattern Recognit. 86 (2019) 27–36.
[11] L. Kriuchkova, I. Tsmokanych, N. Mazur, I. Chernihivskyi, Spectral Characteristics of Intermodulation Emissions during High-Frequency Imposition, in: Cybersecurity Providing in Information and Telecommunication Systems, vol. 3991 (2025) 449–462.
[12] S. Igarashi, et al., Unintentional Radiated Emission from Unshielded Twisted Pair Cable Attributed to Twist Structure. IEICE Commun. Express 2022, 11, pp. 691–696.
[13] NSA, TEMPEST: A Signal Problem. Approved for Release by NSA on 09-07-2007, FOIA Case #51633, 26–30. https://www.nsa.gov/portals/75/documents/news-features/declassified-documents/cryptologic-spectrum/tempest.pdf
[14] D. Berend, Dipoles, Unintentional Antennas and EMC, Serbian J. Electr. Eng. 5 (2008) 31–38.
[15] C. Hare, Fundamentals of Electromagnetic Compliance, 2024. https://incompliancemag.com/article/fundamentals-of-electromagnetic-compliance/
[16] V. Petrivskyi, et al., Development of a Modification of the Method for Constructing Energy-Efficient Sensor Networks using Static and Dynamic Sensors, East.-Eur. J. Enterpr. Technol. 1(115) (2022) 15–23. doi:10.15587/1729-4061.2022.252988
[17] S. Yevseiev, et al., Method of Assessment of Frequency Resolution for Aircraft, East.-Eur. J. Enterpr. Technol. 2(122) (2023) 34–45. doi:10.15587/1729-4061.2023.277898
[18] A. Knyaz, Electrodynamic Signals and Their Processing Systems, Odessa Electrotechnical Institute of Communications, 1988.
[19] A. Rozvadovsky, Calculation of Radiation Characteristics of a Curved Electrical Conductor, Electron. Commun. 1 (2006) 70–75.
[20] V. Shokalo, et al., Fields and Waves in Information Security Systems: Textbook for Higher Education Students, 2012.
[21] Cabinet of Ministers of Ukraine, On Approval of the National Table of Radio Frequency Allocation of Ukraine, vol. 1208, 2005.
[22] L. Kryuchkova, Investigation of the Spatial Characteristics of the Near-Field of Loop Antennas, Modern Inf. Protect. 1 (2018) 17–22.
[23] O. Partyka, A. L. Imoize, AI for Radio Channel Security. Handbook of Cybersecurity Challenges and Solutions for Emerging Technologies (2026). doi:10.1201/9781003640790-16
[24] O. Partyka, A. L. Imoize, C.-T. Li, Cooperative V2X-Based UAV Detection in Rural Transportation Corridors. Drones, 10(2) (2026) 153. doi:10.3390/drones10020153